IEEE Access
Multidisciplinary | Rapid Review | Open Access Journal

Received May 30, 2019, accepted June 26, 2019, date of publication July 1, 2019, date of current version August 7, 2019.

Digital Object Identifier 10.1109/ACCESS.2019.2926057

Control of Hysteretic Systems Through an Analytical Inverse Compensation Based on a NARX Model

WILSON R. LACERDA JUNIOR, SAMIR A. M. MARTINS, ERIVELTON G. NEPOMUCENO, (Member, IEEE), AND MÁRCIO J. LACERDA

Control and Modelling and Control Group (GCOM), Department of Electrical Engineering, Federal University of São João del-Rei, Minas Gerais 36307-334, Brazil

Corresponding author: Samir A. M. Martins (martins@ufsj.edu.br)

This work was supported in part by the Federal University of São João del-Rei, and in part by the Brazilian Agencies CNPq/INERGE, FAPEMIG, and CAPES.

ABSTRACT It has been widely accepted that a hysteretic system can be controlled by combining inverse compensation with feedback. Among the strategies to identify hysteretic systems, data-driven models have been received great attention due to its flexibility and ability to online and adaptive estimation. Nevertheless, less attention has been paid to determine its inversion, which is essential to use such models in control applications. The novelty of this paper is twofold. First, we propose a method to obtain analytically the inverse compensation of a hysteretic system modeled by a Nonlinear Auto-Regressive Model with eXougenous input (NARX) representation with a bounding structure. Second, this paper presents an adapted nonautonomous electronic circuit with rate-independent hysteresis and linear dynamics, which is used as a benchmark to test the proposed methodology. The experimental results have shown the efficiency of the proposed technique.

INDEX TERMS Bounding structure, NARX model, system identification, system with hysteresis, inverse compensation.

I. INTRODUCTION

Hysteresis is a severely nonlinear behavior commonly found in electromagnetic devices, sensors, semiconductors, biomedical, and economic systems, which have memory effects between quasi-static input and output [1]–[3]. It is not uncommon to be an arduous task representing hysteretic systems using physics-based models [4]. More often than not, physics-based models are excessively complex for practical applications involving system characterization, identification or control which require a high level of precision and performance [5]–[7].

A generic framework for controlling hysteretic systems is to use inverse compensation with feedback [8]. The hysteretic effect is canceled employing an inverse for the model, which allows the control of the resulted linear system by, for example, a classic PID control. Hysteresis models can be rate-dependent or rate-independent, concerning the characteristics of the input. The readers are referred to [9]–[12] for more detailed procedures regarding the identification of rate-dependent hysteresis. On the other hand, since fully rate-independent models can describe many processes very well, such as construction structures [13], suspension systems [14], and slab track systems [15], several representations have been employed in last years aiming to methodically describe rate-independent hysteresis behaviors, *e.g.*, neural networks [16]–[18], NARX polynomial [19], [20], phenomenological models [21], fuzzy logic [22] and Bayesian inference [23]. Among the strategies to identify hysteretic systems, data-driven models have been received significant attention due to its flexibility and ability to online and adaptive estimation. In this regard, a computationally efficient method capable of building interpretable models to be effortlessly applied in an inverse compensation and control scenario of symmetric or asymmetric hysteretic loops is still a challenging task.

In particular, a viable alternative for mathematical representation of a hysteretic behavior is the polynomial

The associate editor coordinating the review of this manuscript and approving it for publication was Feiqi Deng.

NARX (Nonlinear Auto-Regressive Model with eXougenous input) [24], [25]. A great effort has been undertaken to search for more accurate and practical models, as can be seen in [26]–[31]. Martins and Aguirre [20] presented an essential step in the actual use of polynomial models. The authors have developed sufficient conditions to reproduce rate-independent hysteresis in identified polynomial NARX.

Despite a considerable amount of research in system identification for hysteretic systems, there remains a need for techniques to determine its inversion, which is essential to use such models in control applications. Some works have been devoted to developing an inverse dynamic, as done by the authors in [32], [33]. However, these works have used black-box identification. Here we have developed an analytical inverse for an identified polynomial NARX. The novelty of this paper is twofold. First, we propose a method to obtain analytically the inverse compensation of a hysteretic system modeled by a NARX representation with a bounding structure. The bounding structure is employed to compensate for the hysteresis phenomenon to make possible the application of linear control techniques in an experimental scenario. Second, this paper presents a nonautonomous electronic circuit, adapted from [37] and [38], but now reproducing rate-independent hysteresis and linear dynamics, which is used as a benchmark to test the proposed methodology. The proposed circuit can be a simple experimental platform to test modeling and control techniques for systems with hysteresis. The proposed circuit is based roughly by RLC circuit and an operational amplifier to produce the hysteretic behavior. The experimental results have shown the potential of the bounding structure to linearize the hysteretic system using a unit-delayed polynomial NARX.

The remainder of this paper is organized as follows. Section II present some definitions. The electronic circuit with hysteresis that has been designed to test the control strategy Section III. The identification procedure applied to the circuit and the hysteresis compensation through the inverse model are also presented in Section III. The results are discussed in Section IV. Section V concludes the study and provides perspectives of future research.

II. BACKGROUND

Before presenting the method and the results, let us introduce a set of definitions and preliminary concepts to a better understanding of this manuscript. This section also presents a brief problem statement for controlling a hysteretic system.

A. PROBLEM STATEMENT

In this section, the problem statement is introduced. One can describe the hysteresis nonlinearity as [34]:

$$y(t) = H[v(t)] \tag{1}$$

where $v(t)$ is the input, $y(t)$ is the output, $x(t)$ is the reference and H stands for the hysteresis operator. The error is given by $e(t) = y(t) - x(t)$. The general aim is to find a control system such as $e(t) \to 0$ as $t \to t_c$, where t_c should be as less as possible. The problem statement is summarized in Fig. 1.

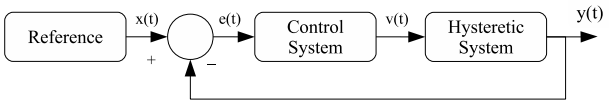

FIGURE 1. Problem statement. Given a hysteretic system, we aim to show a control system to reduce the error to zero. In our approach, the control system is composed of two parts: a linear controller and an inverse compensation.

The design of a control strategy for nonlinear systems with hysteretic behavior is not an easy task. An alternative is to find a compensation function that linearizes the nonlinearity of the system. After this task, the problem relies upon a standard design control, and a PID approach may solve it.

B. PRELIMINARIES

Definition 1 (Hysteresis Loops in Continuous Time $\mathcal{H}_t(\omega)$ [20]): Let x_t be a continuous-time loading-unloading quasi-static signal applied to a continuous-time system and y_t is the system output. $\mathcal{H}_t(\omega)$ denotes a closed loop in the x_t-y_t plane, which shape depends on ω. If the system presents hysteretic nonlinearity, then $\mathcal{H}_t(\omega)$ is denoted as:

$$\mathcal{H}_t(\omega) = \begin{cases} \mathcal{H}_t(\omega)^+, & for\ t_i \le t \le t_m, \\ \mathcal{H}_t(\omega)^-; & for\ t_m \le t \le t_f, \end{cases} \tag{2}$$

where $\mathcal{H}_t(\omega)^+ \neq \mathcal{H}_t(\omega)^-, \forall t \neq t_m$. The time interval given by $t_i \le t \le t_m$ and $t_m \le t \le t_f$ correspond to the regime when x_t is loading and unloading, respectively. $\mathcal{H}_t(\omega)^+$ stands for the part of the loop formed in the x_t-y_t plane, while $t_i \le t \le t_m$ (when x_t is loading) whereas $\mathcal{H}_t(\omega)^-$ is the part of the loop formed in the $x_t - y_t$ plane for $t_m \le t \le t_f$ (when x_t is unloading), as shown in Figure 2.

Remark 2: This work considers the concept of rate-independent hysteresis (RIH). This definition excludes, for example, any memory effect of the viscous type, such as those represented by temporal convolution. Common hysteretic phenomena as in ferromagnetic or elastic materials may not be purely rated independent since viscous-like effects attach to the hysteresis. However, the rate independent component prevails [36].

Definition 3 (Polynomial NARX [24]): Polynomial NARX is a mathematical model based on difference equations and used to describe linear and nonlinear phenomena. The polynomial NARX relates the current output as a function of past inputs and outputs, mathematically described as:

$$y_k = F^{\ell}[y_{k-1}, \ldots, y_{k-n_y}, x_{k-1}, \ldots, x_{k-n_x}] + e_k, \tag{3}$$

where n_y, n_x, are the maximum lags for the system output and input respectively; x_k is the system input and y_k is the system output at discrete time $k \in \mathbb{N}$; e_k stands for uncertainties and possible noise at discrete time k. F^{ℓ} is a polynomial function of input and output regressors with nonlinearity degree $\ell \in \mathbb{N}$.

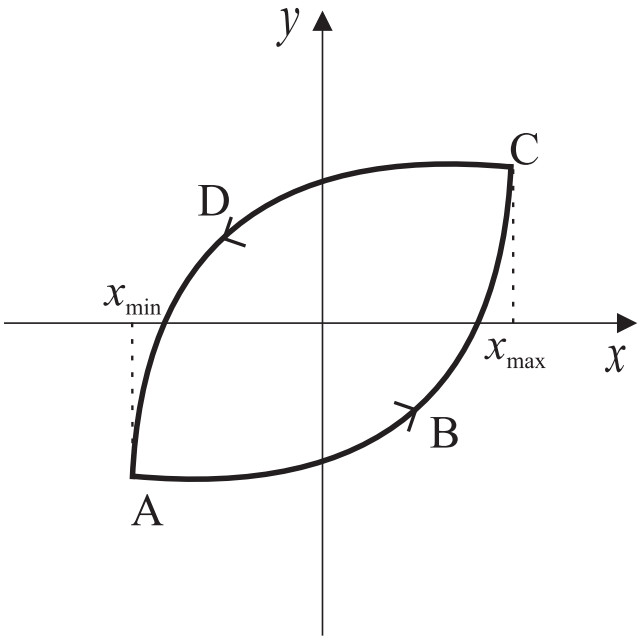

FIGURE 2. Example of a hysteresis curve according to a loading-unloading input signal.

Remark 4: The model (3) can be expanded as a summation of terms with nonlinearity degree in the range $[1\ \ell]$ where each $(p+m)th$ term can contain a factor of order pth in y and mth in x, multiplied by a constant parameter $c_{p,m}(\tau_1,\ldots,\tau_m)$, as follows [20]:

$$y(k) = \sum_{m=0}^{\ell}\sum_{p=0}^{\ell-m}\sum_{\tau_1,\tau_m}^{n_y,n_x} c_{p,m}(\tau_1,\ldots,\tau_{p+m})\prod_{i=1}^{p} y_{k-\tau_i} \times \prod_{i=1}^{m} x_{k-\tau_i} + e_k. \quad (4)$$

In this case, if the summation presented in (4) refers to factors in y, the upper limit is n_y otherwise, if it refers to factors in x it will be n_x.

In steady-state it is reasonable to consider $\overline{y} = y_{k-\tau}, \forall\ \tau = 1,\ldots,n_y$ and $\overline{x} = x_{k-\tau}, \forall\ \tau = 1,\ldots,n_x$. In this way (4) can be rewritten as

$$\overline{y}(k) = \sum_{m=0}^{\ell}\sum_{p=0}^{\ell-m}\left(\sum_{\tau_1,\tau_m}^{n_y,n_x} c_{p,m}(\tau_1,\ldots,\tau_{p+m})\right)\overline{y}^p\overline{x}^m, \quad (5)$$

giving room for the Definitions presented in what follows.

Definition 5 (Term Cluster and Cluster Coefficients [35]): A set of terms of the form $y_{k-i}^p x_{k-j}^m$ to $m+p \le \ell$, where $i = 1,\ldots,n_y$ and $j = 1,\ldots,n_x$ are time delays, is called a term cluster and can be written as $\Omega_{y^p x^m}$.

The constant $\sum_{\tau_1,\tau_m}^{n_y,n_x} c_{p,m}(\tau_1,\ldots,\tau_{p+m})$ in (5) is the cluster coefficient of a set of terms $\Omega_{y^p x^m}$, which contains terms of the form $y(k-i)^p x(k-j)^m$. The cluster coefficients are denoted by $\sum_{y^p x^m}$.

Definition 6 (Bounding Structure $\mathcal{H}$ [20]): Let $\mathcal{H}_t(\omega)$ be the system hysteresis. $\mathcal{H} = \lim_{\omega\to 0}\mathcal{H}_t(\omega)$ is defined as the bounding structure that delimits the system hysteresis loop $\mathcal{H}_t(\omega)$.

Lemma 7 (RIH in Polynomial NARX [20]): Consider a polynomial NARX excited by a loading-unloading quasi-static signal. If the model has one real and stable equilibrium point whose location depends on input and loading/unloading regime, then the polynomial exhibits a RIH hysteresis loop $\mathcal{H}_t(\omega)$ in the x-y plane. The proof of this Lemma is in [20].

III. BOUNDING STRUCTURE FOR IDENTIFICATION AND CONTROL OF AN ELECTRONIC CIRCUIT WITH HYSTERESIS

The method used to identify and to control the hysteretic system based on the bounding structure of a polynomial NARX [20] is detailed. However, first, the proposed electronic circuit with hysteresis is presented.

A. DYNAMIC CIRCUIT WITH HYSTERESIS

Based on the works of [37] and [38], an experimental electronic circuit with hysteresis has been used for identification and control as depicted in Figure 3. Although the basic structure of the circuit uses the same principle established on above-cited works, in order to reproduce low frequencies rate-independent hysteresis the input frequency range and parameters were adjusted. Additionally, to cascade a new dynamic behavior, the circuit structure is extended. Two conditions can explain the occurrence of hysteresis in this type of circuit: i) it has a non-monotonous non-linear static DC conduction point; ii) it has an energy storage element that accommodates fast energy transfers. The topologies of the operational amplifiers used, which have characteristics of negative resistance, reaches the first condition. Hence, hysteresis occurs by controlling the characteristic of the non-monotonous non-linear conduction point using the input variable of the amplifier, resulting in multiple values of the output variable with discontinuous jumps characteristics. These discontinuities result from a fast energy transfer process. Using the energy storage elements in order to control voltage and current characteristics (capacitor and inductor, respectively) ensure the condition (ii) for the occurrence of hysteresis.

Circuit parameters are given in Table 1. One should notice that simply modifying the input resistance R_1 changes the shape of the hysteresis loop. In this sense, the proposed system can reproduce different hysteretic behavior. Besides, a dynamical behavior is cascaded to the hysteresis phenomenon by a second order RLC circuit.

B. IDENTIFICATION OF THE PROPOSED SYSTEM

Firstly, experimental tests and data acquisition were performed using the research facility of Laboratory of Studies in Modeling and Control in Federal University of São João del-Rei, Brazil. A NI DAQPad-6259 Data Acquisition Card equipped with 32 analog input ($16-Bit$ analog to digital resolution and sample rate of $1.25\ MS/s$) and 4 analog output ($16-Bit$ digital to analog converter resolution and sample rate of $2.86\ MS/s$) has been used to produce the input signal for

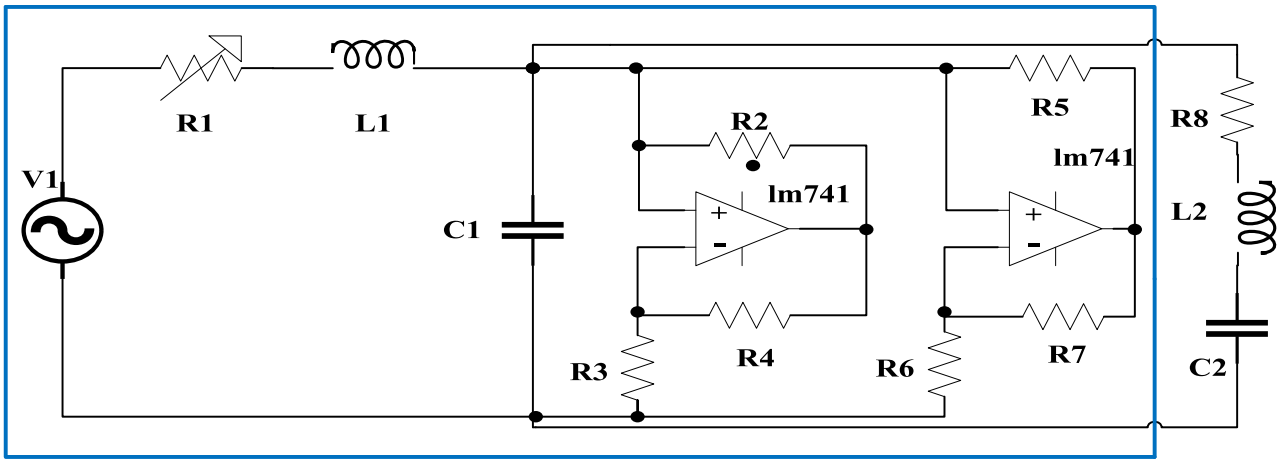

FIGURE 3. Circuit diagram of the system with hysteresis. The blue frame represents the part of the circuit that presents hysteretic behavior.

TABLE 1. Parameters of the proposed system.

Component	R_1	R_2	R_3	R_4	R_5	R_6	R_7	R_8	L_1	L_2	C_1	C_2
Value	$3.5k\Omega$	$22k\Omega$	$3.3k\Omega$	$22k\Omega$	330Ω	$22k\Omega$	330Ω	220Ω	$5mH$	$9.7mH$	$10nF$	$0.82\mu F$

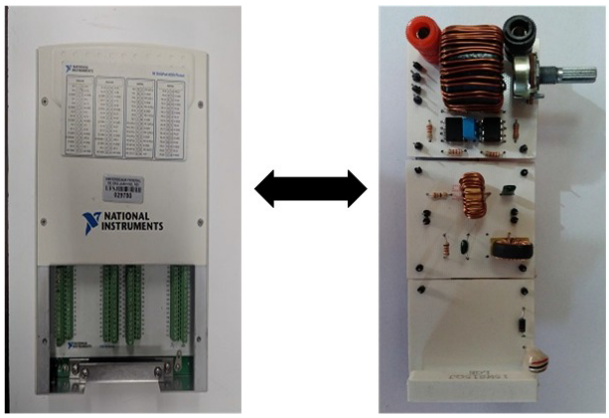

FIGURE 4. Photography of the electronic circuit with hysteresis and the DAQ device used in the experiment.

identification purpose and the control input for the hysteretic system. A white Gaussian noise sequence filtered by a low pass Blackman-Harris FIR filter with 6Hz cutoff frequency has been used as an input signal to excite the electronic circuit with hysteresis. The sample rate is 800 *Hz*.

Figure 4 shows the setup composed by the DAQ device and the custom-built electronic circuit.

A sufficient condition for hysteresis in the polynomial NARX is the existence of a multi-function of the first input difference $\phi(\Delta x_k)$ in the model structure. In this way, $\phi(\Delta x_k)$ is the first model regressor. Delays higher than one are excluded from the structure selection procedure, because they significantly decrease the model performance when representing hysteresis [17], [19]. The model structure that can represent the system behavior is developed checking the influence of each term cluster and its respective coefficients on the bounding structure $\mathcal{H}$. Given the a priori knowledge of the hysteresis loop the set of term clusters that approximates the hysteretic behavior is chosen to build the final model. Since the linear-in-the-parameter model (3) can be generically represented in the compact matrix form

$$y = \Psi\Theta + \Xi, \tag{6}$$

where Ψ is a vector of some combinations of the regressors and Θ the vector of parameters, the parameters are estimated using the Least Squares (LS) method by minimizing the residual sum of squares $\Xi^\top\Xi$, given by:

$$\hat{\Theta} = (\Psi^\top\Psi)^{-1}\Psi^\top y. \tag{7}$$

The performance of the model is quantified by the normalized RMSE (Root Mean Squared Error) in a specific data set. The normalized RMSE can be expressed by:

$$\text{RMSE} = \frac{\sqrt{\sum_{k=1}^{N}(y(k)-\hat{y}(k))^2}}{\sqrt{\sum_{k=1}^{N}(y(k)-\bar{y})^2}}, \tag{8}$$

where $\hat{y}(k)$ the model output and $\bar{y}$ the mean of the measured output $y(k)$.

C. HYSTERESIS COMPENSATION USING THE BOUNDING STRUCTURE $\mathcal{H}$

The modeling and compensation based on NARX model are advantageous since the NARX methodology allows for the inclusion of lagged terms and interactions between them resulting in uncomplicated, interpretable and efficient models which parameters can be estimated to fit the main aspects of a particular hysteresis loop. Also, the NARX representation with a bounding structure allows the model to describe

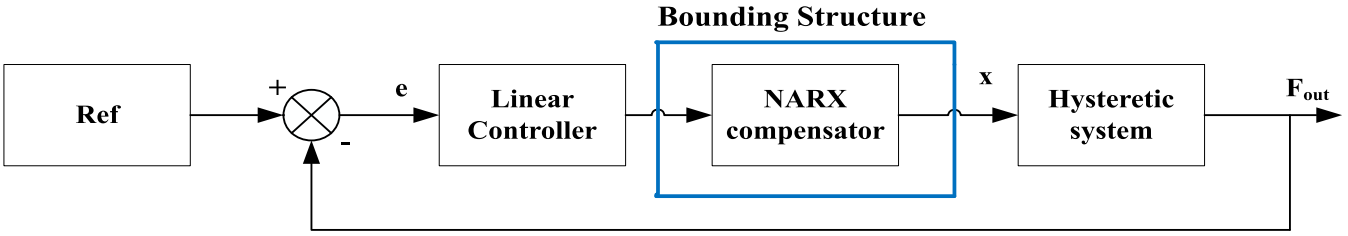

FIGURE 5. Control and compensation diagram. *Ref*, x, F_{out} and e are the input reference, the compensation input, the controlled output and the error between *Ref* and F_{out}.

different symmetric, asymmetric, and saturated input-output hysteresis behaviors.

The bounding structure $\mathcal{H}$ allows the data-driven identification of a polynomial NARX model with sufficient conditions to represent hysteresis. In this respect, to achieve the compensation of the nonlinear phenomenon, the inverse of the polynomial NARX is developed.

In this context, an inverse model for the system described by (3) can be defined as

$$x_k = G^{\ell}[x_{k-1}, ..., x_{k-n_x}, y_{k-1}, \ldots, y_{k-n_y}] + e_k, \tag{9}$$

where n_y, n_x, are the maximum lags of the output and input, respectively and $G^{\ell}[\cdot]$ is the nonlinear function.

By isolating the input regressor x of the obtained polynomial NARX, the hysteresis compensation law is achieved, which is based on the current reference to be tracked ($y_{ref,k} = F_{ref,k}$) and its future values $y_{ref,k+1}$. One should notice that the inverse model is not causal since it uses the information of future desired outputs to estimate the present input. However, future values of y_{ref} are already known. Therefore, the inverse compensation can be done in a straightforward manner using the same identified model, with no necessity to estimate additional parameters.

An illustrative example is presented in what follows.

Example 8: Let us consider the polynomial NARX of a magnetorheological damper obtained in [20]:

$$y_k = ay_{k-1} + bx3_{k-1} + cx2_{k-1}x1_{k-1} + dx3_{k-1}x2_{k-1}y_{k-1}, \tag{10}$$

where the output y_k is the hysteretic force, the inputs $x1_k$ and $x2_k$ are the input voltage and velocity and $x3_k = \text{sign}(x2_k)$, represents the sign of the velocity. Thus, model (10) can be rewritten as:

$$y_k = ay_{k-1} + b\text{sign}(x2_{k-1}) + cx2_{k-1}x1_{k-1} + d\text{sign}(x2_{k-1})x2_{k-1}y_{k-1}. \tag{11}$$

Isolating x_1 in (11) and considering $y_k = y_{ref_k}$ the compensation input is described as:

$$x1_k = \frac{1}{cx2_k}\left[y_{ref_{k+1}} - ay_{ref_k} - b\text{sign}(x2_k) - d\text{sign}(x2_k)y_{ref_k}\right]. \tag{12}$$

Due to the simplicity of the polynomial NARX and the ability of the bounding structure $\mathcal{H}$ to reproduce the system hysteresis, the inverse model can be used for hysteresis compensation. Once the inverse polynomial NARX (9) linearizes the system, linear control techniques can manage the desired performance for the closed-loop system. In this study, a second-order transfer function approximates the dynamics of the compensated system, and a PID controller is used to control the system dynamics as depicted in Figure 5.

IV. RESULTS

In this Section, the bounding structure of a polynomial NARX has been applied to compensate hysteresis in an electronic circuit. First, the identified model is obtained from empirical data. Afterward, it is shown why the obtained model reproduces hysteresis and the operation region where hysteresis occurs. The identified model is used to compensate the hysteresis and, to conclude, a PID controller is tuned based on the compensated system. The experimental results are presented and discussed at the end of this section.

A. IDENTIFIED POLYNOMIAL AND BOUNDING STRUCTURE $\mathcal{H}$ ANALYSIS

Using the presented approach, the obtained model structure is composed by the term clusters Ω_y, Ω_{x_1}, Ω_{x_2}, Ω_{x_3}, Ω_{x_3y}, $\Omega_{x_3x_2y}$, where y is the system output, x_1 is the input signal, x_2 is the multi-valued function of the input signal $\phi(\Delta x1_k) = \text{sign}(x1_k - x1_{k-1})$ and x_3 is the sign of the output $\phi(\Delta y_k) = \text{sign}(y_k - y_{k-1})$. As presented in Section III, a unit-delayed regressor of each cluster have been used to compose the hysteresis model. The identified model is given by the following polynomial:

$$\begin{aligned} y_k \;=\; & 0.3790y_{k-1} + 0.2721x1_{k-1} + 0.2166x2_{k-1} \\ & +0.4874x3_{k-1} - 0.0574y_{k-1}x3_{k-1} \\ & -0.2749y_{k-1}x2_{k-1}x3_{k-1}. \end{aligned} \tag{13}$$

Figure 6a depicts the free run simulation of the model identified from experimental data. As can be observed, the model performance is satisfactory when representing the system dynamics. Figure 6b presents the polynomial hysteresis loops contrasted with the hysteresis from the electronic circuit. The computed RMSE for this model using the validation data set is 0.1263.

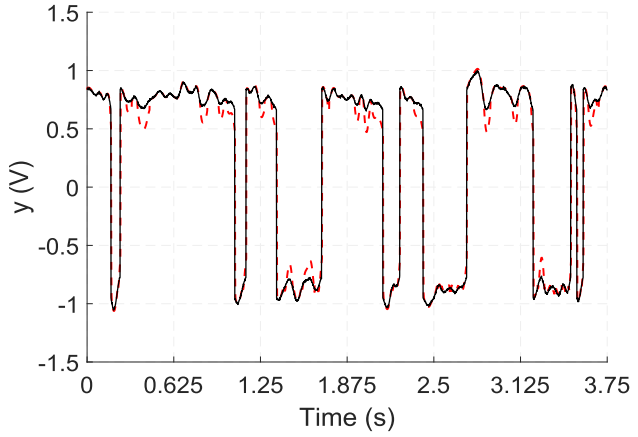

(a) Validation of the NARX model. (-)Experimental purposed system, (- -) NARX model.

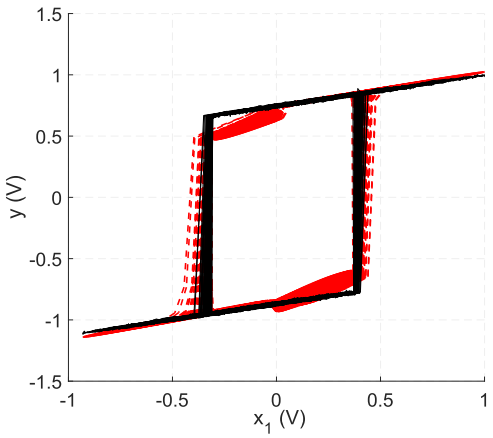

(b) Hysteresis loop of the model. (-) indicate the experimental data and (- -) indicates the data of the model.

FIGURE 6. Free run simulation and hysteresis loop of the model.

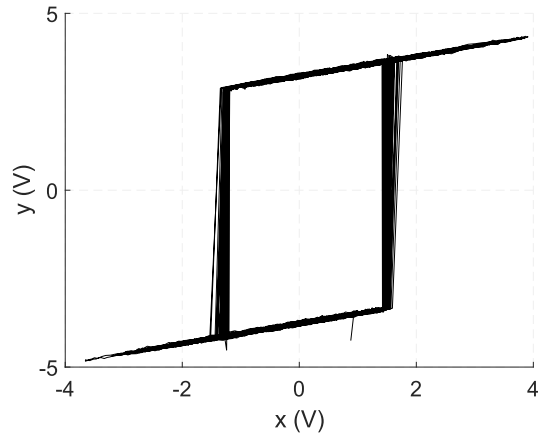

(a) Hysteresis behavior of the purposed system.

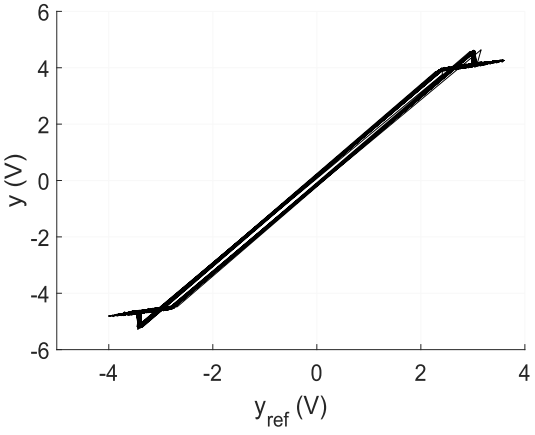

(b) Anticipatory compensation system following the reference signal. The horizontal axis represents the reference output (y_{ref}) and the vertical axis represents the system output (y).

FIGURE 7. Hysteresis compensation using the inverse model.

As introduced in the preliminary concepts, model (13) yields hysteresis if at least one asymptotically stable equilibrium point depends on the input loading-unloading regime. During the loading and unloading regime, $\phi(\Delta x_k) = sign(\Delta x_k)$ will be a constant $\bar{\phi}$ whose value will depend on Δx_k. To verify the equilibria local stability a steady-state analysis can be performed as:

$$\bar{y}(\bar{x}_1, \bar{x}_2, \bar{x}_3) = \begin{cases} \dfrac{\Sigma_\phi + \Sigma_{x_1}\bar{x}_1 + \Sigma_{x_3}\bar{x}_3}{1 - \Sigma_y - \Sigma_{yx_3}\bar{x}_3 + \Sigma_{y\phi x_3}\bar{x}_3}, & \text{loading;} \\ \dfrac{-\Sigma_\phi + \Sigma_{x_1}\bar{x}_1 + \Sigma_{x_3}\bar{x}_3}{1 - \Sigma_y - \Sigma_{yx_3}\bar{x}_3 - \Sigma_{y\phi x_3}\bar{x}_3}, & \text{unloading;} \end{cases} \tag{14}$$

where $\Sigma_y = 0.3790$, $\Sigma_{x_1} = 0.2721$, $\Sigma_{x_3} = 0.4874$, $\Sigma_\phi = 0.2166$, $\Sigma_{yx_3} = -0.0574$ and $\Sigma_{y\phi x_3} = -0.2749$. The local stability condition for these equilibria are $-1 < \Sigma_y + \Sigma_{yx_3}\bar{x}_3 + \Sigma_{y\phi x_3}\bar{x}_2\,\bar{x}_3 < 1$. Rearranging the values of Σ_y, Σ_{yx_3} e $\Sigma_{y\phi x_3}$ yields:

$$\frac{1.3790}{\text{-}0.0574\text{-}0.2749\bar{x}_2} < \text{-}\bar{x}_3 < \frac{\text{-}0.6210}{\text{-}0.0574\text{-}0.2749\bar{x}_2}. \tag{15}$$

Under loading regime ($x_2 = 1$), the stability condition is reached under $-1.8687 < x_3 < 4.1498$. Since data are normalized, this condition indicates that the equilibria are locally stable under the region of interest. For unloading regime, the equilibria remain for $-6.3402 < x_3 < 2.8551$ adopting an analogous analysis. Because the identified model satisfies these conditions, it produces hysteresis.

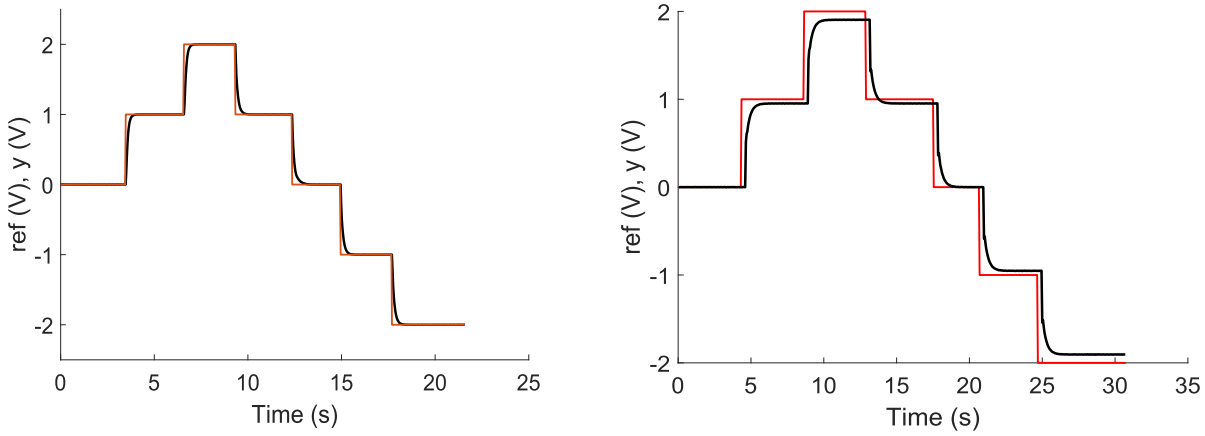

(a) Controller performance using heuristic tuning. The parameters are $K_p = 2.23$, $K_i = 0.14$ and $K_d = 4.25$.

(b) Controller performance without hysteresis compensation by means of the inverse model. The parameters are $K_p = 2.23$, $K_i = 0.14$ and $K_d = 4.25$.

FIGURE 8. Controller performance with compensation and without hysteresis compensation. In red the reference signal and in black the trajectory of the controlled system.

B. HYSTERESIS COMPENSATION

According to Section III-C, in order to compensate hysteresis, model (13) can be rewritten as:

$$\begin{aligned} x_{1_k} = \frac{1}{0.2721}[&y_{ref_{k+1}} - 0.3790 y_{ref_k} - 0.4874 \text{sign}(\Delta y_{ref_k}) \\ &+ 0.0574 y_{ref_k} \text{sign}(\Delta y_{ref_k}) - 0.2166 \text{sign}(x_{1_k}) \\ &+ 0.2749 \text{sign}(\Delta x_{1_k}) \text{sign}(\Delta y_{ref_k}) y_{ref_k}]. \end{aligned} \quad (16)$$

As can be seen in (16), it is known that x_{1_k} depends on $\text{sign}(\Delta x_{1_k})$. Since it is a function of the same variable at the same sample time k, it is not possible to obtain the value of x_{1_k}. To overcome this limitation, we take in this paper $\text{sign}(\Delta x_{1_k}) \approx \text{sign}(\Delta x_{1_{k-1}})$ to compute x_{1_k}.

The reference y_{ref} serves as the input of the compensated system to check the hysteresis compensation. In this regard, Figure 7a depicts the system original hysteresis and Figure 7b shows its compensation.

Once the hysteresis compensation linearizes the system, any linear controller can be associated to improve the control system. In this work, a PID controller is the selected technique. Two cases have been investigated to tune the parameters: i) the parameters are adjusted heuristically. ii) a second-order transfer function, identified from the compensated system, is used to tune the PID parameters, composing the entire control system presented in Figure 5. The following section summarizes the results.

C. PID CONTROLLER HEURISTICALLY TUNED

Figure 8a reports the result of the heuristically tuned PID controller, considering the system compensated by the inverse model. In this case, the controller parameters have been adjusted in real time until the controller achieves satisfactory performance. The parameters in this case are $K_p = 2.23$, $K_i = 0.14$ and $K_d = 4.25$. With this adjustment, the response did not show any overshoot. In addition, the same parameters are applied in a non-compensated scenario (Figure 8b). As can be observed, the performance without the use of the inverse model to compensate the hysteresis is not satisfactory, since there is a delay in the system response and considerable error in steady state. This response can be explained due to the reference signal is operating in a transition band of the hysteresis loop.

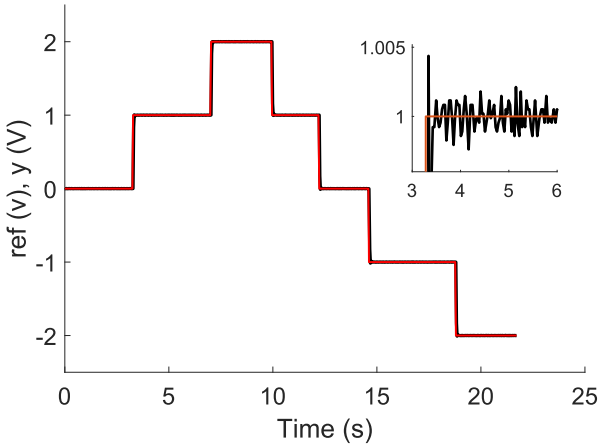

FIGURE 9. Controller performance using PID Tuner tuning. PID parameters: $K_p = 3.27$, $K_i = 0.35$ and $K_d = 7.69$.

D. PID CONTROLLER TUNED BY SOFTWARE

The second-order transfer function identified from data of the linearized system is defined by:

$$H(s) = \frac{0.01592s + 0.05524}{s^2 + 0.142s + 0.05544}. \quad (17)$$

The identified second-order model was validated using the normalized RMSE presented by Equation (8), presenting 0.0390 as a computed value. After the linearized system

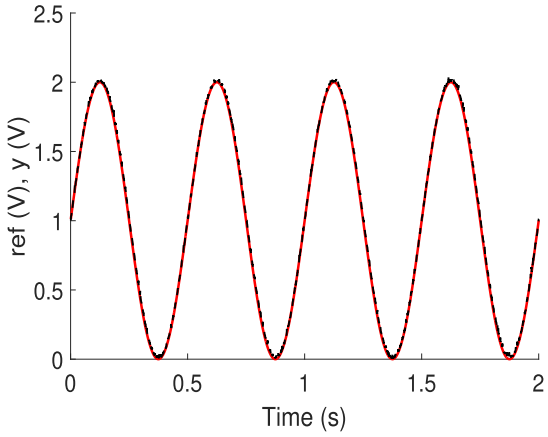

(a) Reference 1: $2 + 2sin(4\pi t)$.

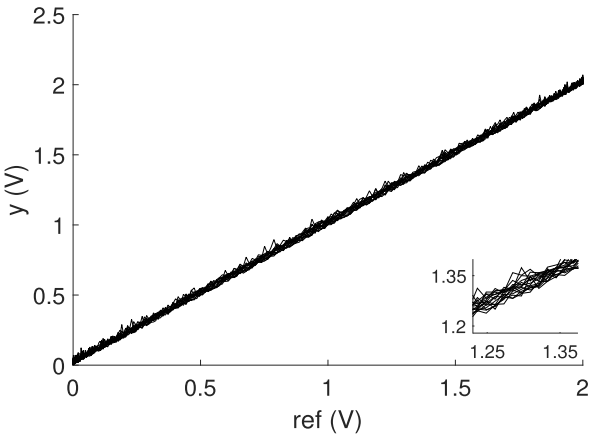

(b) Respective suppressed hysteresis loop.

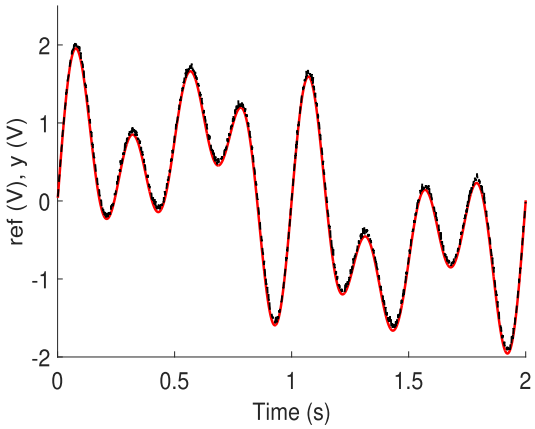

(c) Reference: $4sin(1\pi t) + 1.2sin(4\pi t) + 1.5sin(8\pi t) + 0.8sin(6\pi t)$.

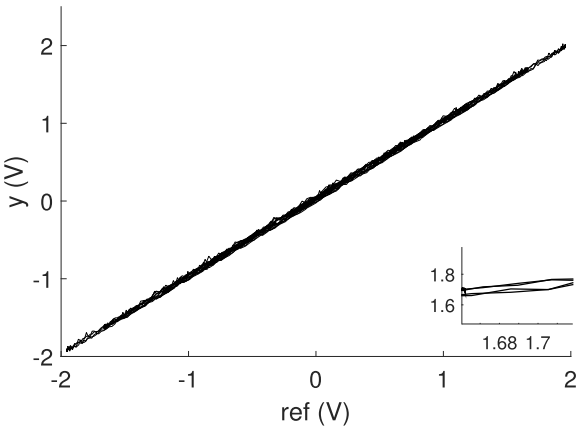

(d) Respective compensated hysteresis loop.

FIGURE 10. Response of the proposed controller. Reference signal is depicted in red and the controlled system output is shown in black.

TABLE 2. Performance due to a different tuning of the PID controller.

	K_p	K_i	K_d	Rise Time (s)		Settling time		Steady-state error	
				$ref = 2V$	mean	$ref = 2V$	mean	$ref = 2V$	mean
Software-based PID tunning	3.27	0.35	7.69	0.030	0.029	0.100	0.104	0.05%	0.05%
Heuristic PID tuning	2.23	0.14	4.25	0.330	0.339	0.359	0.366	0.16%	0.15%
Without compensation	2.23	0.14	4.25	0.690	0.682	0.740	0.742	3.82%	3.51%

identification, the PID Tuner tool from Matlab was used to tune the controller. Figure 9 present the closed-loop control system using software-based tuning for PID parameters.

Table 2 summarizes the results obtained both by using heuristic or software-based tuning. In this respect, the improvement is evident because of the use of the bounding structure $\mathcal{H}$ in the system control process as an analytical hysteresis compensation tool. Table 2 reports that the output converges to the reference signal under PID control combined with bounding structure $\mathcal{H}$. Moreover, the PID controller generates a faster response when tuned by software than the heuristic tuning method, as also expected.

Additionally, in order to demonstrate the performance of the proposed control strategy, two reference signals with more complex characteristics were applied, respectively: a sinusoidal signal with DC offset, $2 + 2sin(4\pi t)$, and a sine wave with both amplitude and frequency varying, $4sin(1\pi t) + 1.2sin(4\pi t) + 1.5sin(8\pi t) + 0.8sin(6\pi t)$. For the former case the PID parameters are $K_p = 3.58$, $K_i = 0.44$, and $K_d = 6.05$; for the latter case the PID parameters are

$K_p = 4.33$, $K_i = 0.78$, and $K_d = 7.89$. Fig. 10 depicts the system output regarding the aforementioned reference inputs. As can be seen in Fig. 10(b) and (d), the hysteresis could be properly suppressed in both cases using the bounding structure $\mathcal{H}$ when the reference signal is composed by more complex signals. The experimental results demonstrate the good tracking performance of the proposed method, being the $RMSE = 0.01$ for the first complex signal and $RMSE = 0.04$ for the second one.

V. CONCLUSION

This paper has presented an analytical method to obtain the inverse compensation for control of a hysteretic system. There is no difficulty in obtaining the inverse compensation as the model of a hysteretic system is based on a NARX model and a bounding structure $\mathcal{H}$ first introduced in [20].

We have also implemented an electronic circuit which has been used to acquire real data with rate-independent hysteresis. All the classic steps of system identification have been applied to obtain a model with a bounding structure, which allows modeling with a good agreement with the hysteretic properties. After that, the inverse compensation has been calculated to allow the control design for a linearized plant. In this respect, a PID controller has been implemented in a physical system with hysteresis associated with the inverse model of the hysteresis loop. The parameters of the controller have been adjusted using the PID Tuner tool from a transfer function model of the system. Besides, a heuristic tuning of the controller has been performed for purposes of comparison with a control approach without compensation using the inverse model.

The performance of the obtained model can be evaluated in an experimental scenario of hysteresis compensation using the inverse model, whose objective is to compensate the hysteretic nonlinearities using an anticipatory architecture. Since the structural complexity of the NARX models is small, it is possible to obtain the inverse model in a significantly simpler way than in phenomenological models. Also, it is crucial to emphasize that the inverse model is essential for satisfactory performance in the control of the system. As can be observed, the control of the system without compensation has not achieved convincing results.

Future research will address the direct identification of the inverse hysteresis model for application in anticipatory control; depth analysis of the influence of term clusters on the formation of the bounding structure $\mathcal{H}$, making it possible to obtain an even simpler form of the model. Finally, rate-dependent hysteresis will be discussed to shed new light onto system identification and control of hysteretic systems using polynomial NARX.

REFERENCES

[1] I. Ahmad, "Two degree-of-freedom robust digital controller design with Bouc-Wen hysteresis compensator for piezoelectric positioning stage," *IEEE Access*, vol. 6, pp. 17275–17283, Mar. 2018. doi: 10.1109/ACCESS.2018.2815924.

[2] F. Ikhouane and J. Rodellar, *Systems with Hysteresis: Analysis, Identification and Control Using the Bouc-Wen Model*. Hoboken, NJ, USA: Wiley, 2007, pp. 1–12.

[3] N. Aguirre, F. Ikhouane, J. Rodellar, and R. Christenson, "Parametric identification of the Dahl model for large scale MR dampers," *Struct. Control Health Monit.*, vol. 19, no. 3, pp. 332–347, Feb. 2012. doi: 10.1002/stc.434.

[4] M. A. Janaideh, J. Mao, S. Rakheja, W. Xie, and C.-Y. Su , "Generalized Prandtl-Ishlinskii hysteresis model: Hysteresis modeling and its inverse for compensation in smart actuators," in *Proc. IEEE 47th Conf. Decis. Control*, Dec. 2008, pp. 5182–5187. doi: 10.1109/CDC.2008.4739202.

[5] M. Ismail, F. Ikhouane, and J. Rodellar, "The hysteresis bouc-wen model, a survey," *Arch. Comput. Methods Eng.*, vol. 16, no. 2, pp. 161–188, Feb. 2009. doi: 10.1007/s11831-009-9031-8.

[6] T. Sireteanu, M. Giuclea, A.-M. Mitu, and G. Ghita, "A genetic algorithms method for fitting the generalized Bouc-Wen model to experimental asymmetric hysteretic loops," *J. Vib. Acoust.*, vol. 134, no. 4, pp. 041007–041010, May 2012. doi: 10.1115/1.4005845.

[7] A. Amthor, S. Zschaeck, and C. Ament, "High precision position control using an adaptive friction compensation approach," *IEEE Trans. Autom. Control*, vol. 55, no. 1, pp. 274–278, Jan. 2010. doi: 10.1109/TAC.2009.2036307.

[8] R. V. Iyer and X. Tan, "Control of hysteretic systems through inverse compensation," *IEEE Control Syst.*, vol. 29, no. 1, pp. 83–99, Feb. 2009. doi: 10.1109/MCS.2008.930924.

[9] J. Gan and X. Zhang, "An enhanced Bouc-Wen model for characterizing rate-dependent hysteresis of piezoelectric actuators," *Rev. Sci. Instrum.*, vol. 90, no. 11, Jan. 2019, Art. no. 115002. doi: /10.1063/1.5087005.

[10] M. A. Janaideh, C.-Y. Su and S. Rakheja, "Development of the rate-dependent Prandtl–Ishlinskii model for smart actuators," *Smart Mater. Struct.*, vol. 17, no. 3, Apr. 2008, Art. no. 035026. doi: 10.1088/0964-1726/17/3/035026.

[11] J. Gan, X. Zhang, and H. Wu, "A generalized Prandtl-Ishlinskii model for characterizing the rate-independent and rate-dependent hysteresis of piezoelectric actuators," *Rev. Sci. Instrum.*, vol. 87, no. 3, Mar. 2016, Art. no. 035002. doi: 10.1063/1.4941941.

[12] M. Al Janaideh and O. Aljanaideh, "Further results on open-loop compensation of rate-dependent hysteresis in a magnetostrictive actuator with the Prandtl-Ishlinskii model," *Mech. Syst. Signal Process.*, vol. 104, no. 1, pp. 835–850, May 2018. doi: 10.1016/j.ymssp.2017.09.004.

[13] F. Weber, "Semi-active vibration absorber based on real-time controlled MR damper," *Mech. Syst. Signal Process.*, vol. 46, no. 2, pp. 272–288, Jun. 2014. doi: 10.1016/j.ymssp.2014.01.017.

[14] S. Dutta, S.-M. Choi, and S.-B. Choi, "A new adaptive sliding mode control for Macpherson strut suspension system with magneto-rheological damper," *J. Intell. Mater. Syst. Struct.*, vol. 27, no. 20, pp. 2795–2809, Apr. 2016. doi: 10.1177/1045389X16641221.

[15] R. Li, W. Mu, T. Sun, X. Li, and X. Wang, "Benchmark study of a small-scale slab track system with squeeze-mode magnetorheological fluid isolators," *J. Intell. Mater. Syst. Struct.*, vol. 29, no. 1, pp. 52–61, May 2018. doi: 10.1177/1045389X17705219.

[16] S. L. Xie, Y. H. Zhang, C. H. Chen, and X. N. Zhang, "Identification of nonlinear hysteretic systems by artificial neural network," *Mech. Syst. Signal Process.*, vol. 34, nos. 1–2, pp. 76–87, Jan. 2013. doi: 10.1016/j.ymssp.2012.07.015.

[17] H. Du, J. Lam, and N. Zhang, "Modelling of a magneto-rheological damper by evolving radial basis function networks," *Eng. Appl. Artif. Intell.*, vol. 19, no. 8, pp. 869–881, Dec. 2006. doi: 10.1016/j.engappai.2006.02.005.

[18] M. Khalid, R. Yusof, M. Joshani, H. Selamat, and M. Joshani, "Nonlinear identification of a magneto-rheological damper based on dynamic neural networks," *Comput.-Aided Civil Infrastruct. Eng.*, vol. 29, no. 3, pp. 221–233, Feb. 2013. doi: 10.1111/mice.12005.

[19] A. Leva and L. Piroddi, "NARX-based technique for the modelling of magneto-rheological damping devices," *Smart Mater. Struct.*, vol. 11, no. 1, pp. 79–88, Feb. 2002. doi: 10.1088/0964-1726/11/1/309.

[20] S. A. M. Martins and L. A. Aguirre, "Sufficient conditions for rate-independent hysteresis in autoregressive identified models," *Mech. Syst. Signal Process.*, vol. 75, no. 15, pp. 607–617, Jan. 2016. doi: 10.1016/j.ymssp.2015.12.031.

[21] X.-X. Bai, F.-L. Cai, and P. Chen, "Resistor-capacitor (RC) operator-based hysteresis model for magnetorheological (MR) dampers," *Mech. Syst. Signal Process.*, vol. 117, pp. 157–169, Feb. 2019. doi: 10.1016/j.ymssp.2018.07.050.

[22] K. K. Ahn, M. A. Islam, and D. Q. Truong, "Hysteresis modeling of magneto-rheological (MR) fluid damper by self tuning fuzzy control," in *Proc. IEEE Int. Conf. Control, Automat. Syst.*, Oct. 2008, pp. 2628–2633. doi: 10.1109/iccas.2008.4694300.

[23] K. Worden and J. J. Hensman, "Parameter estimation and model selection for a class of hysteretic systems using Bayesian inference," *Mech. Syst. Signal Process.*, vol. 32, pp. 153–169, Oct. 2012. doi: 10.1016/j.ymssp.2012.03.019.

[24] I. J. Leontaritis and S. A. Billings, "Input-output parametric models for non-linear systems Part I: Deterministic non-linear systems," *Int. J. Control*, vol. 41, no. 2, pp. 303–328, Jan. 1985. doi: 10.1080/0020718508961129.

[25] S. A. Billings, *Nonlinear System Identification: NARMAX Methods in the Time, Frequency, and Spatio-Temporal Domains*, 1st ed. Hoboken, NJ, USA: Wiley, 2013, pp. 17–59.

[26] R. Dong, Y. Tan, Y. Xie, and K. Janschek, "Recursive identification of micropositioning stage based on sandwich model with hysteresis," *IEEE Trans. Control Syst. Technol.*, vol. 25, no. 1, pp. 317–325, Jan. 2017. doi: 10.1109/TCST.2016.2542004.

[27] J. Noël, A. F. Esfahani, G. Kerschen and J. Schoukens, "A nonlinear state-space approach to hysteresis identification," *Mech. Syst. Signal Process.*, vol. 84, no. 1, pp. 171–184, Feb. 2017. doi: 10.1016/j.ymssp.2016.08.025.

[28] J. Gunnar, E. Wernholt, G. Hovland, and T. Brogardh, "Nonlinear grey-box identification of linear actuators containing hysteresis," in *Proc. IEEE Int. Conf. Robot. Automat.*, Orlando, FL, USA, May 2006, pp. 1818–1823. doi: 10.1109/ROBOT.2006.1641970.

[29] F. Zhang, K. M. Grigoriadis, and I. J. Fialho, "Linear parameter-varying control for active vibration isolation systems with stiffness hysteresis," *J. Vib. Control*, vol. 15, no. 4, pp. 527–547, Feb. 2009. doi: 10.1177/1077546308096105.

[30] B. N. M. Truong, D. N. C. Nam, and K. K. Ahn, "Hysteresis modeling and identification of a dielectric electro-active polymer actuator using an APSO-based nonlinear Preisach NARX fuzzy model," *Smart Mater. Struct.*, vol. 22, no. 9, Aug. 2013, Art. no. 095004. doi: 10.1088/0964-1726/22/9/095004.

[31] Y. Liu, J. Shan, Y. Meng, and D. Zhu, "Modeling and identification of asymmetric hysteresis in smart actuators: A modified MS model approach," *IEEE/ASME Trans. Mechatronics*, vol. 21, no. 1, pp. 38–43, Feb. 2016. doi: 10.1109/TMECH.2015.2500905.

[32] P.-Q. Xia, "An inverse model of MR damper using optimal neural network and system identification," *J. Sound Vib.*, vol. 266, no. 5, pp. 1009–1023, Oct. 2003. doi: 10.1016/s0022-460x(02)01408-6.

[33] C.-C. Chang and L. Zhou, "Neural network emulation of inverse dynamics for a magnetorheological damper," *J. Struct. Eng.*, vol. 128, no. 2, pp. 231–239, Feb. 2002. doi: 10.1061/(asce)0733-9445(2002)128:2(231).

[34] G. Zhang, C. Zhang, and C. Wang, "Iterative learning control of hysteresis in piezoelectric actuators," *Math. Problems Eng.*, vol. 2014, May 2014, Art. no. 856706. doi: /10.1155/2014/856706.

[35] L. A. Aguirre and S. A. Billings, "Improved structure selection for non-linear models based on term clustering," *Int. J. Control*, vol. 62, no. 3, pp. 569–587, 1995. doi: 10.1080/00207179508921557.

[36] A. Visintin, "Genesis of hysteresis," in *Differential Models of Hysteresis* (Applied Mathematical Sciences), vol. 111. Berlin, Germany: Springer, 1994.

[37] A. S. Elwakil, S. Ozoguz, and R. Jad'a, "Explaining hysteresis in electronic circuits: Robust simulation and design examples," in *Proc. IEEE 13th Int. Conf. Electron., Circuits Syst.*, Nice, France, Dec. 2006, pp. 244–247. doi: 10.1109/ICECS.2006.379771.

[38] K. Murali, M. Lakshmanan, and L. O. Chua, "The simplest dissipative nonautonomous chaotic circuit," *IEEE Trans. Circuits Syst. I, Fundam. Theory Appl.*, vol. 41, no. 6, pp. 462–463, Jun. 1994. doi: 10.1109/81.295246.

WILSON R. LACERDA JUNIOR received the B.Sc. degree in electrical engineering from the Federal University of São João del-Rei (UFSJ), Brazil, where he is currently pursuing the master's degree in modeling and control of dynamical systems and also a member of Control and Modelling Group (GCOM). His research interests include identification of nonlinear systems, NARMAX methods, nonlinear time series analysis and forecasting, neural networks, and chaotic systems.

SAMIR A. M. MARTINS received the B.Sc. and M.Sc. degrees in engineering from the Federal University of São João del-Rei and the Ph.D. degree in electrical engineering from the Federal University of Minas Gerais. He has been an Adjoint Professor with the Electrical Engineering Department, Federal University of São João del-Rei, since 2013. His recent research interests include nonlinear system identification, circuit and systems control, and hysteresis modeling and control.

ERIVELTON G. NEPOMUCENO received the B.Sc. degree from UFSJ and the Ph.D. degree in electrical engineering from UFMG, Brazil. From 2013 to 2014, he was a Postdoctoral Research Fellow with the Intelligent Systems and Networks Group, Imperial College London. He is currently an Associate Professor with Federal University of São João del-Rei (UFSJ) and the Leader of Control and Modelling Group (GCOM). His research interests include chaos, complex systems, computer arithmetic, interval arithmetic, and system identification. He is a member of the Brazilian Association of Automatica and the IEEE Circuit and Systems Society (IEEE CAS). In 2018, he was appointed as a member of the Technical Committee on Nonlinear Circuits and Systems (TC-NCAS) of the IEEE CAS Society. He is an Associate Editor of the IEEE LATIN AMERICA TRANSACTIONS and *Journal of Biomedical Research and Reviews*.

MÁRCIO J. LACERDA received the Ph.D. degree in electrical engineering from the School of Electrical and Computer Engineering (FEEC), University of Campinas, Campinas, Brazil, in 2014. From 2012 to 2013, he was a Visitor at the Laboratoire d' Analyse et d' Architecture des Systèmes, Toulouse, France. From 2014 to 2015, he was with FEEC, as a Postdoctoral Associate, and from 2015 to 2016, he was with the Aerospace Engineering and Mechanics Department, University of Minnesota, Minneapolis, USA, as a Postdoctoral Associate. Since 2016, he is currently an Assistant Professor with the Electrical Engineering Department, Federal University of São João del-Rei. His research interests include uncertain systems, robust control, filtering theory, and polynomial systems.